

Electronic Supplementary Information

Cocrystals/salt of 1-naphthalene acetic acid and utilizing Hirshfeld surface calculations for acid-aminopyrimidine synthon

Utsav Garg^a, Yasser Azim^{*a}, Aranya Kar^b, Chullikkattil P. Pradeep^b

^aDepartment of Applied Chemistry, Z.H. College of Engineering & Technology, Aligarh Muslim University, Aligarh, 202002, Uttar Pradesh, India.

^bSchool of Basic Sciences, Indian Institute of Technology Mandi, Kamand, 175005, Himachal Pradesh, India.

*Corresponding author

Content

Table S1. Characteristic FT-IR bands of pure components (NAA, 2-AP, 2-A-4,6-DMP, 2,4,6-TAP) and their cocrystals/salt (NAA-2-AP, NAA-2-A-4,6-DMP and (NAA)⁻(2,4,6-TAP)⁺)

Table S2. Percent contribution of strong and weak interactions in crystal packing of starting materials and all the three reported cocrystal/salt.

Figure S1. FTIR spectrum (500–4000 cm⁻¹) of starting materials and ground mixture of (a) NAA-2-AP (b) NAA-2A-4,6-DMP (c) (NAA)⁻(2,4,6-TAP)⁺.

Figure S2. PXRD patterns of starting materials and ground mixtures of (a) NAA-2-AP (b) NAA-2A-4,6-DMP (c) (NAA)⁻(2,4,6-TAP)⁺

Figure S3. Graphical comparison of weak interactions among starting materials and all the three reported cocrystals/salts.

Figure S4. A view of Hirshfeld surface mapped over curvedness for (a) NAA-2-AP (b) NAA-2A-4,6-DMP (c) (NAA)⁻(2,4,6-TAP)⁺.

Figure S5. A view of Hirshfeld surface mapped over shape-index for (a) NAA-2-AP (b) NAA-2A-4,6-DMP (c) (NAA)⁻(2,4,6-TAP)⁺.

Figure S6. A view of Hirshfeld surface mapped over calculated electrostatic potential in the range -0.077 to +0.056 atomic units for (a) NAA-2-AP (b) NAA-2A-4,6-DMP (c) (NAA)⁻(2,4,6-TAP)⁺.

Figure S7. Colour-coded total interaction energies calculated for (a) NAA-2-AP (b) NAA-2A-4,6-DMP (c) (NAA)⁻(2,4,6-TAP)⁺. The individual electrostatic, polarization, dispersion and exchange-repulsion energies with scale factors of 1.057, 0.740, 0.871 and 0.618, respectively are also shown.

Table S1

Characteristic FT-IR bands of pure components (NAA, 2-AP, 2-A-4,6-DMP, 2,4,6-TAP) and their cocrystals/salt ((NAA)⁻(2,4,6-TAP)⁺)

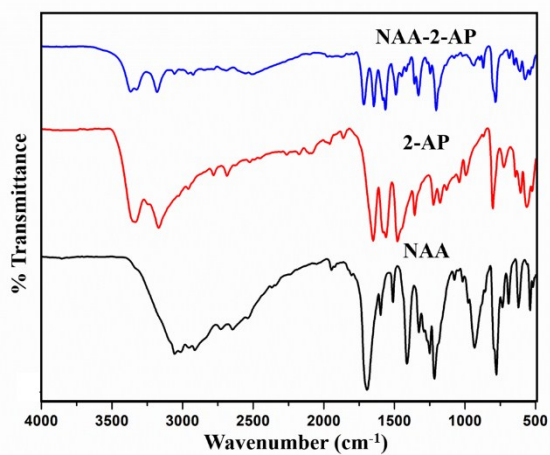
Sample	Wavenumber (in cm ⁻¹)				
	C=O stretching (Acid)	C-O stretching (Acid)	N-H stretching (Pyrimidine)	O-H stretching (Acid)	C=N stretching (Pyrimidine)
NAA	1691	1216	×	3051	×
2-AP	×	×	3326	×	1557
2-A-4,6-DMP	×	×	3406	×	1595
2,4,6-TAP	×	×	3314	×	1575
NAA-2-AP	1714	1200	3340	3175	1562
NAA-2-A-4,6-DMP	1662	1170	3333	3162	1590
(NAA) ⁻ (2,4,6-TAP) ⁺	1377	1377	3329	×	1545

Table S2

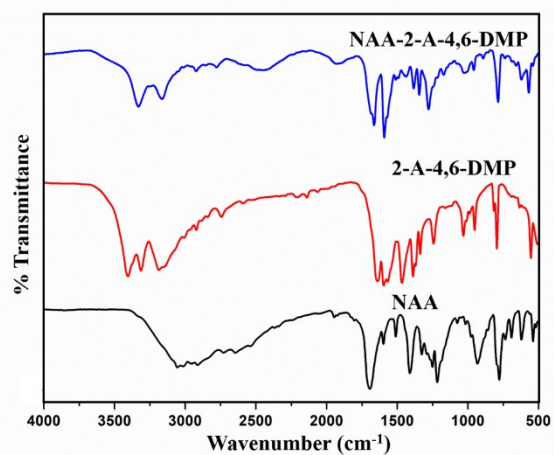
Percent contribution* of strong and weak interactions in crystal packing of starting materials and all the three reported cocrystal/salt.

*Calculated using *CrystalExplorer17*

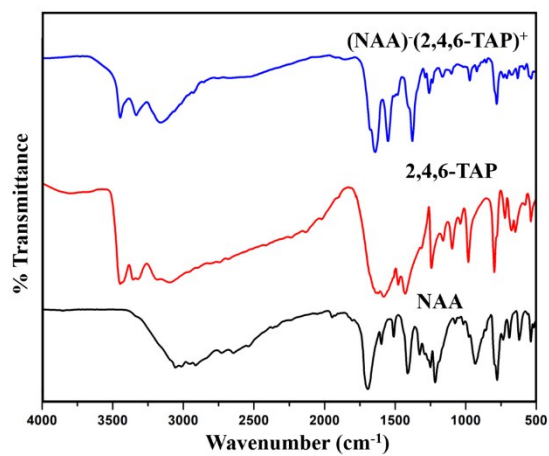
Compound	Strong interactions (% contribution)			Weak interactions (% contribution)								
	N...H	O...H	Total	H...H	C...H	C...N	C...O	C...C	N...O	N...N	O...O	Total
NAA	×	21.9	21.9	43.5	32.8	×	0.4	1.0	×	×	0.5	78.2
2-AP	34.1	×	34.1	42.6	17.9	2.8	×	1.7	×	1	×	66
2-A-4,6-DMP	23.1	×	23.1	62.9	6.3	2.7	×	5	×	0.0	×	76.9
2,4,6-TAP	29.4	×	29.4	46.1	13.4	4.6	×	2.6	×	3.9	×	70.6
NAA-2-AP	25.7	10	35.7	39.1	23.9	0.5	0	0.3	0.4	0	0	64.2
NAA-2-A-4,6-DMP	13.9	13.6	27.5	49	14	5	0	3.2	0	1.2	0	72.4
(NAA) ⁻ (2,4,6-TAP) ⁺	20.6	17.3	37.9	39.6	17.6	0.9	1.1	1.9	1.1	0.0	0.0	62.2



(a)



(b)



(c)

Figure S1. FTIR spectrum (500–4000 cm⁻¹) of starting materials and ground mixture of (a) NAA-2-AP (b) NAA-2A-4,6-DMP (c) (NAA)(2,4,6-TAP)⁺.

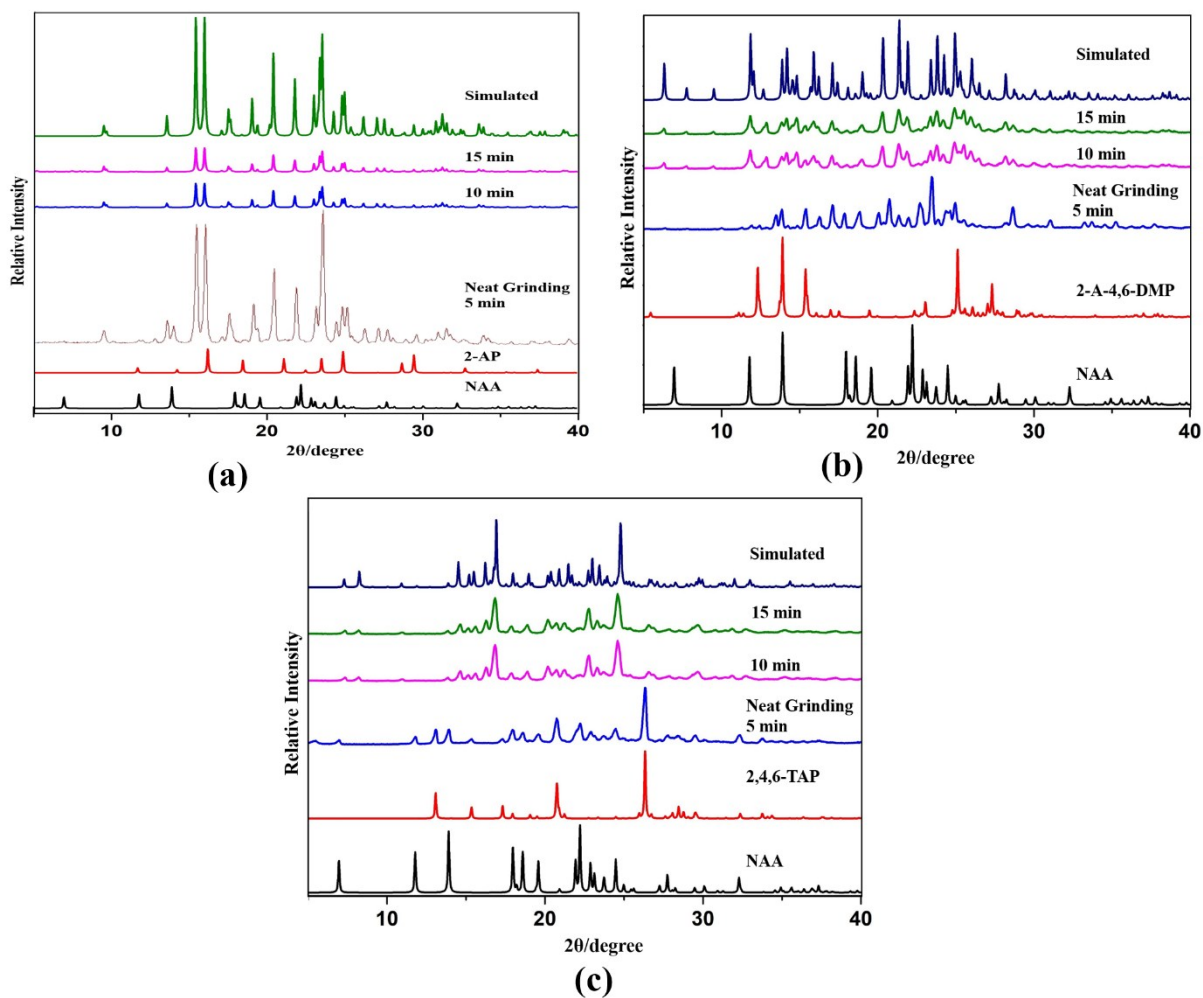


Figure S2. PXRD patterns of starting materials and ground mixtures of (a) NAA-2-AP (b) NAA-2A-4,6-DMP (c) (NAA)-(2,4,6-TAP)⁺.

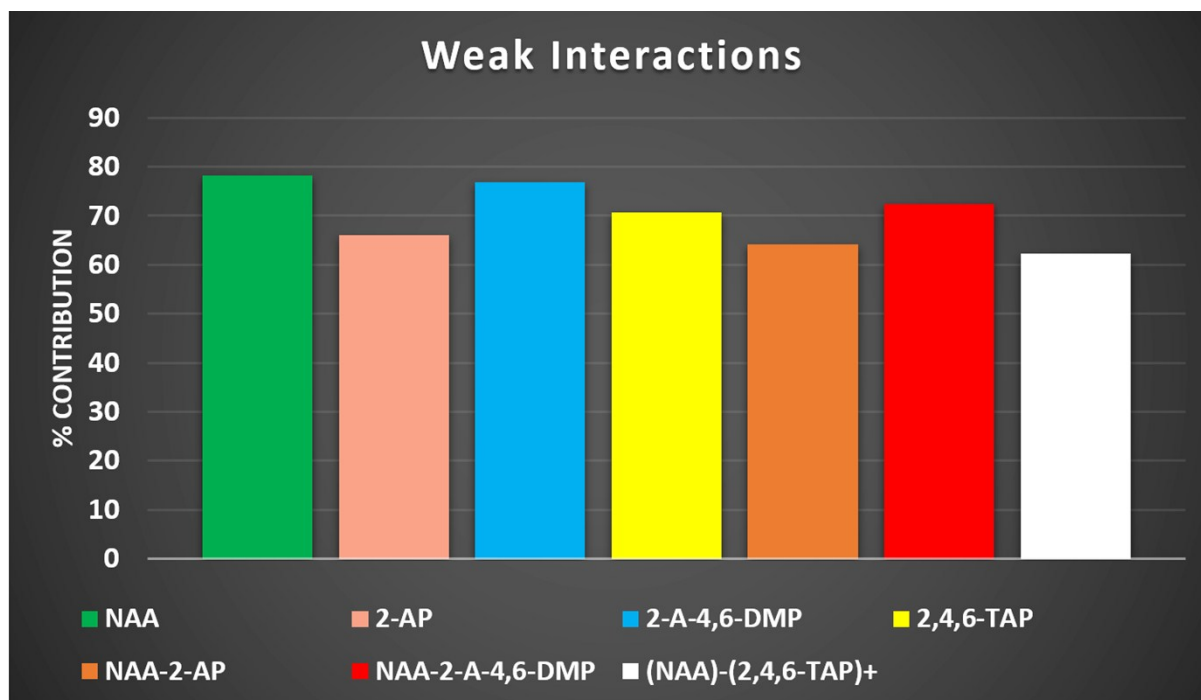


Figure S3. Graphical comparison of weak interactions among starting materials and all the three reported cocrystals/salts.

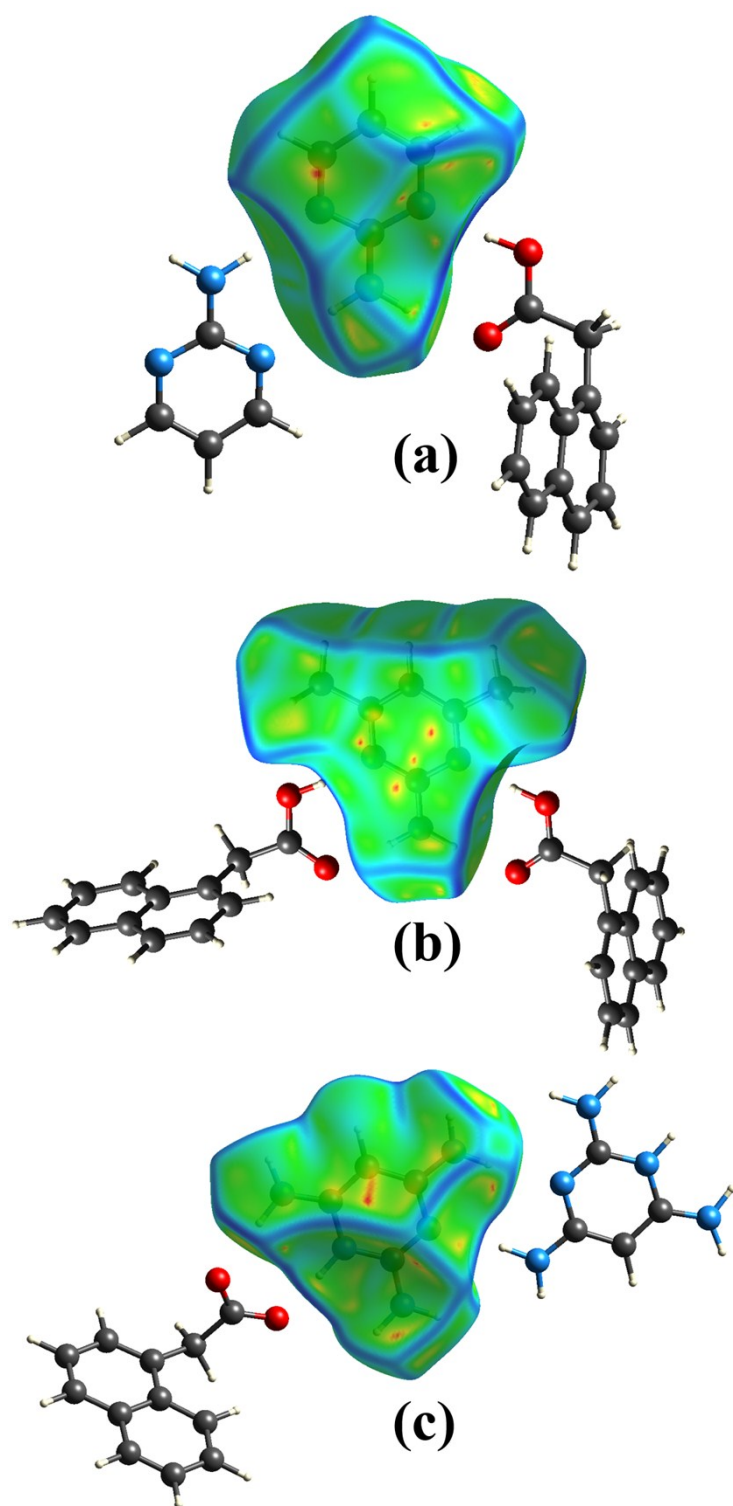


Figure S4. A view of Hirshfeld surface mapped over curvedness for (a) NAA-2-AP (b) NAA-2A-4,6-DMP (c) (NAA)-(2,4,6-TAP)⁺. The flat region indicates $\pi \cdots \pi$ stacking interactions.

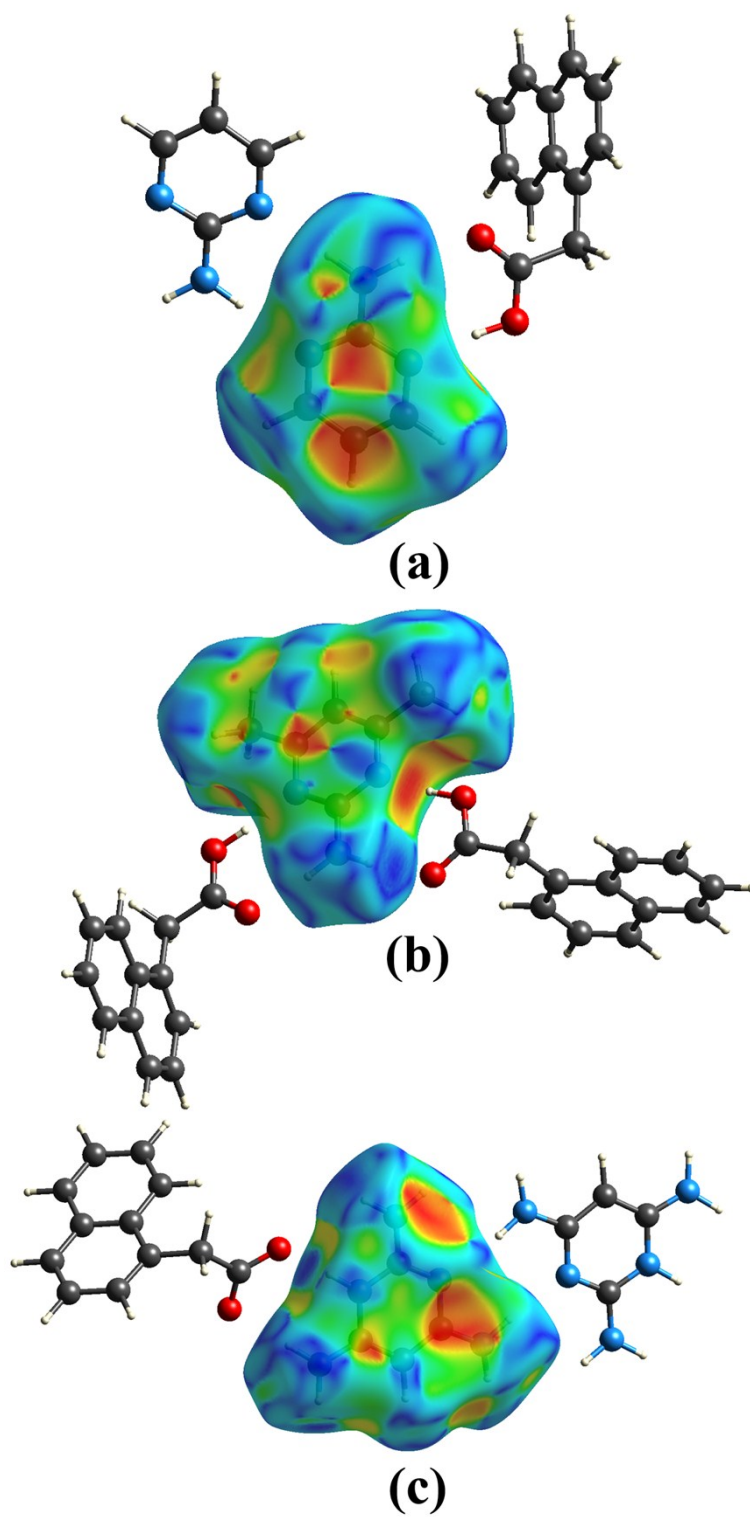


Figure S5. A view of Hirshfeld surface mapped over shape-index for (a) NAA-2-AP (b) NAA-2A-4,6-DMP (c) (NAA)-(2,4,6-TAP)⁺. The red and blue triangles indicate the presence of C—H \cdots π interaction and $\pi\cdots\pi$ stacking.

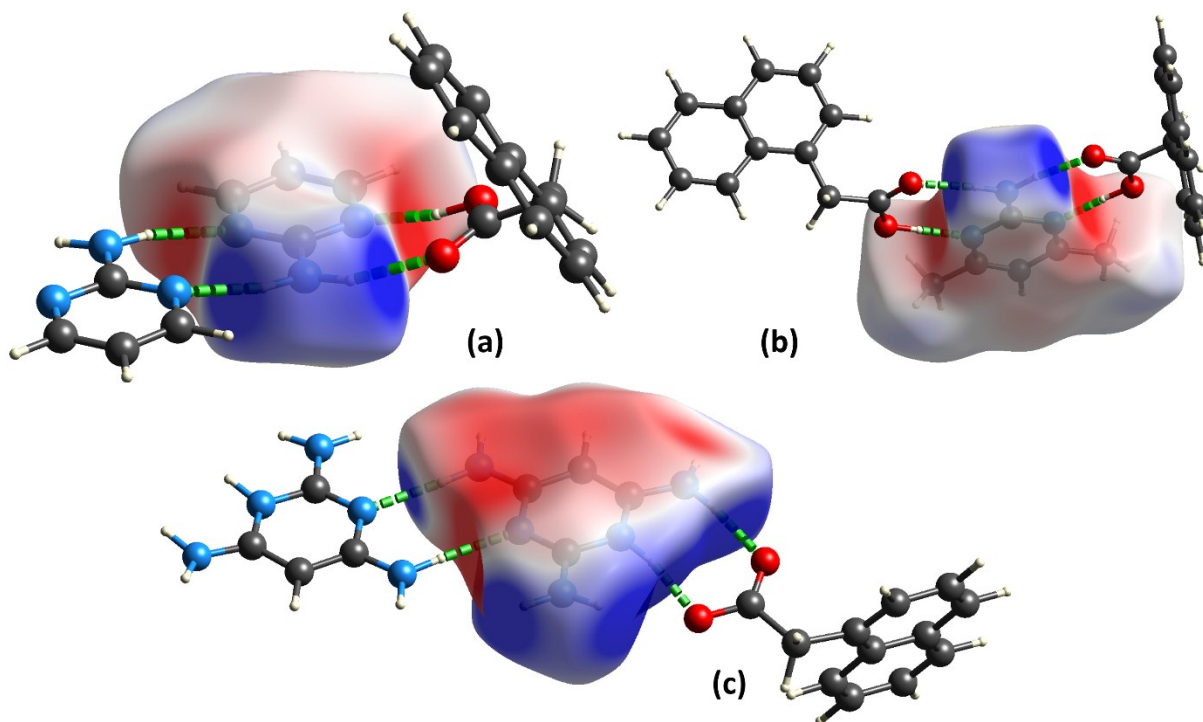


Figure S6. A view of Hirshfeld surface mapped over calculated electrostatic potential in the range -0.077 to $+0.056$ atomic units for (a) NAA-2-AP (b) NAA-2A-4,6-DMP (c) (NAA)⁻(2,4,6-TAP)⁺. The blue and red regions represent positive and negative electrostatic potential respectively.

	N	Symop	R	Electron Density	E_ele	E_pol	E_dis	E_rep	E_tot
	1	-	6.48	B3LYP/6-31G(d,p)	-98.0	-21.8	-15.0	107.0	-66.7
	1	-x, -y, -z	5.49	B3LYP/6-31G(d,p)	-57.2	-12.5	-14.2	57.0	-46.8
	1	-	6.45	B3LYP/6-31G(d,p)	-2.8	-0.5	-15.9	11.7	-9.9
	1	-	7.69	B3LYP/6-31G(d,p)	-4.2	-0.6	-7.5	8.2	-6.2
	1	-	5.81	B3LYP/6-31G(d,p)	-6.3	-0.8	-18.2	15.6	-13.4

(a)

	N	Symop	R	Electron Density	E_ele	E_pol	E_dis	E_rep	E_tot
	1	-	7.44	B3LYP/6-31G(d,p)	-117.2	-27.6	-19.0	138.3	-75.5
	1	-	7.21	B3LYP/6-31G(d,p)	-116.8	-27.3	-18.6	139.1	-74.0
	1	-	7.43	B3LYP/6-31G(d,p)	-0.1	-0.4	-4.8	0.5	-4.2
	1	-x, -y, -z	3.81	B3LYP/6-31G(d,p)	-1.1	-1.8	-33.3	14.3	-22.6
	1	-	6.05	B3LYP/6-31G(d,p)	-6.5	-0.7	-22.2	19.4	-14.7

(b)

	N	Symop	R	Electron Density	E_ele	E_pol	E_dis	E_rep	E_tot
	1	-	7.29	B3LYP/6-31G(d,p)	-76.2	-13.4	-15.0	125.0	-26.4
	1	-	7.20	B3LYP/6-31G(d,p)	-16.6	-5.2	-10.0	24.8	-14.8
	1	-	7.23	B3LYP/6-31G(d,p)	-6.4	-2.4	-14.9	10.8	-14.9
	1	-x, -y, -z	6.34	B3LYP/6-31G(d,p)	-43.7	-15.0	-18.4	65.0	-33.1
	1	-	5.68	B3LYP/6-31G(d,p)	-11.9	-4.9	-20.7	15.8	-24.5

(c)

Figure S7. Colour-coded total interaction energies calculated for (a) NAA-2-AP (b) NAA-2-A-4,6-DMP (c) (NAA)⁻(2,4,6-TAP)⁺. The individual electrostatic, polarization, dispersion and exchange-repulsion energies with scale factors of 1.057, 0.740, 0.871 and 0.618, respectively are also shown.